TWO SMOOTH ANALOGS FOR A PIECEWISE-SMOOTH 1 PREDATOR–2 PREY SYSTEM

Sofia H. Piltz * Lauri Harhanen † Mason A. Porter‡ Philip K. Maini §

25th October 2016

Abstract

We construct two smooth analogs of an existing piecewise-smooth dynamical system model for freshwater plankton that consists of an adaptively feeding predator and its two prey types. We relax the assumption of "discontinuous" prey switching and thereby allow a gradual change in the predator's diet choice as a response to prey abundance, and we then fit the parameter to empirical data to infer the slope of the gradual diet switch. We smooth out the piecewise-smooth dynamical system in two different ways: (1) by using the hyperbolic tangent function; and (2) by incorporating a parameter that changes abruptly across the discontinuity in a piecewise-smooth system as a system variable that is coupled to the population dynamics. We conduct linear stability analyses and compare the model behavior of the two smooth models with that of the piecewise-smooth model. We then compare model predictions quantitatively to data for freshwater plankton and show that the two smooth analogs fit the data well when the smooth transition is steep, supporting the simplifying assumption of a discontinuous prey switching behavior in this scenario.

1 Introduction

Piecewise-smooth dynamical systems are a class of discontinuous systems that describe behavior using smooth dynamics of variables that alternate with abrupt events [6,8]. Piecewise-smooth descriptions can arise in two different ways. First, abrupt events occur naturally in numerous systems and can arise from situations such as collisions, impacts, friction, and switches with on-states and off-states in electrical circuits [8]. Second, piecewise-smooth systems are also used to approximate strongly-nonlinear terms, such as sigmoidal or cubic functions, in models for systems that incorporate transitions between two or more states.

Piecewise-smooth dynamics occur in a wide variety of applications [8]. In engineering, these applications include, for example, models for mechanical oscillators such as a rocking block (see, e.g, [17]), relay-feedback systems, in which an electrically operated switch is used to control a process or an electromechanical system (see, e.g., [9]), or systems exhibiting dry-friction (see, e.g., [16]), to mention only few. One important family of biological applications of piecewise-smooth systems are gene regulatory networks, in which transcription factors either initiate or inhibit the production of proteins after some threshold concentration has been reached [5,12]. Another is conceptual climate models, where an abrupt change in a piecewise-smooth system can represent a transition between different regimes in, for example, large-scale ocean circulation [43] or the Earth's reflectivity due to ice cover [1].

In a piecewise-smooth dynamical system, phase space is divided into two or more smooth regions by one or more *switching manifolds* that mark transitions between the regions. All of the dynamical behavior that can occur in smooth dynamical systems can also occur in piecewise-smooth systems as

*Department of Applied Mathematics and Computer Science, Technical University of Denmark, Asmussens allé, Bygning 303B, 2800 Kongens Lyngby, Denmark and Department of Mathematics, University of Michigan, 2074 East Hall, Ann Arbor, Michigan, 48109-1043, USA (piltz@umich.edu).

†Department of Applied Mathematics and Computer Science, Technical University of Denmark, Asmussens allé, Bygning 303B, 2800 Kongens Lyngby, Denmark (lauri.harhanen@alumni.aalto.fi).

‡Oxford Centre for Industrial and Applied Mathematics, Mathematical Institute, University of Oxford, Andrew Wiles Building, Radcliffe Observatory Quarter, Woodstock Road, Oxford, OX2 6GG, UK; CABDyN Complexity Centre, University of Oxford, Oxford, OX1 1HP, UK; and Department of Mathematics, University of California, Los Angeles, Los Angeles, California 90095, USA (mason@math.ucla.edu).

§Wolfson Centre for Mathematical Biology, Mathematical Institute, University of Oxford, Andrew Wiles Building, Radcliffe Observatory Quarter, Woodstock Road, Oxford, OX2 6GG, UK and CABDyN Complexity Centre, University of Oxford, Oxford, OX1 1HP, UK. (maini@maths.ox.ac.uk).

well, especially for bifurcations that occur far from a switching manifold [8]. Piecewise-smooth systems also exhibit novel dynamics that do not occur in smooth systems [8]. The theory for piecewise-smooth systems is developing rapidly, and one can gain important insights into the analysis of both "naturally occurring" piecewise-smooth systems (e.g., engineering systems with impacts or relays) and in justifying their use as simplifying approximations (for nonlinear interactions) by approximating a piecewise-smooth system as a smooth dynamical systems (for which analytical and numerical theory is plentiful [13]). In general, one can derive different smooth approximations to the same piecewise-smooth system [7, 24, 28]. Comparing such systems with both each other and their associated piecewise-smooth system is crucial for understanding of the correspondence and transition between a piecewise-smooth system and its smooth analogs.

One can "smooth out" a discontinuity of a piecewise-smooth system using a differentiable transition function of sigmoidal form [7]. One possibility, which we use for our smoothing in Section 2.1, is to use a hyperbolic tangent as a transition function. Alternatively, one can "regularize" a piecewise-smooth dynamical system [28] into a singular perturbation problem [15,25] that includes multiple time scales by "blowing up" the switching boundary [41,44]. (In this work, we do not consider regularizations including multiple time scales. However, we note that a subset of us introduce a time scale separation to one of the smooth analogs of a piecewise-smooth system obtained in this paper and analyze the resulting multiple time scale system in [36].) As a result, trajectories of a vector field at the discontinuity boundary (i.e., a *sliding vector field*) become solutions of a *reduced problem* (i.e., slow flow generated by the slow vector field), and one can approximate the discontinuous vector field of the piecewise-smooth system near the switching boundary by a *layer problem* (i.e., fast flow generated by the fast vector field) [41, 44] in a dynamical system with multiple time scales [28]. In addition, one can include nonlinear terms when obtaining a smooth dynamical system by smoothing out an instantaneous switch by using the method developed in [22, 23]. These nonlinear terms take into account small effects that are observable only during the switch and vanish in the corresponding piecewise-smooth system [24]. Conversely, one can represent a smooth dynamical system as a piecewise-smooth system by using the technique of "pinching", in which a region of phase space is collapsed to form the discontinuity boundary [4].

In this paper, we use an example from ecology to investigate the justification of using a piecewise-smooth system as a simplifying approximation of a smooth system. With our example, we also aim to increase understanding of the correspondence between piecewise-smooth and smooth dynamical systems with no separation of time scales[1]. In our example, we examine the ecological concept of *prey switching*, in which a predator adaptively changes habitat or diet in response to changes in its two or more prey abundances [34][2]. One can model prey switching with smooth dynamical systems by considering either density-dependent switching [2] or density-independent switching [37], or by using information on which prey type was last consumed [50, 51]. In contrast, a piecewise-smooth system arises when one assumes that a switch in a predator's feeding behavior depends on prey abundances and then examines which diet composition maximizes its rate of energy intake [27, 29, 30, 42]. Similarly, using a piecewise-smooth system, a subset of us have suggested recently that prey switching is a possible mechanistic explanation for the dynamics observed in freshwater plankton [35].

On one hand, it is unclear whether there exist "discontinuous predators" who switch their feeding strategy instantaneously, as the model in [35] assumes. On the other hand, we have not found evidence for any of the possible smooth transition functions that one can choose to model prey switching. Therefore, by using the same data set as in [35], we illustrate an example situation in which it is justified to use a piecewise-smooth system as a simplifying approximation of a smooth dynamical system. We show that the piecewise-smooth model in [35] is a mathematically consistent limit of two smooth analogs, which we construct by (1) using a hyperbolic tangent as a transition function from one diet choice to the other and (2) incorporating a parameter that changes abruptly across the discontinuity in the model in [35] as a system variable with dynamics on a time scale comparable to that of the population dynamics of the predator and its two prey. In the second construction, we examine a system with one more dimension than the corresponding piecewise-smooth system. In [36], a subset of us introduce a time scale difference to the second construction. This is a prerequisite for comparing not only the qualitative but also the quantitative behavior in the different models (i.e., piecewise-smooth, smooth, and fast-slow) to each other.

[1] We note that a subset of us analyze a smooth dynamical system similar to the four-dimensional smooth system presented in this work and including a time scale separation in [36].

[2] Note that prey switching in a system of 1 predator and 1 prey refers to a situation in which predation is low at low prey densities but saturates quickly at a high value when prey is abundant. In such a scenario, one can model the predator–prey interaction using a Holling type-III functional response [11, 18].

The remainder of our paper is organized as follows. In Section 2, we present and briefly discuss the equations for the 1 predator–2 prey piecewise-smooth model from [35]. The piecewise-smooth system includes a tilted switching manifold that marks a transition between two smooth parts of phase space. Biologically, these parts represent the predator's adaptive feeding behavior and its two different diet choices: on one side of the switching manifold, the predator's diet consists solely of its preferred prey; on the other side, it consists of the alternative prey. We consider two possible regularizations of the model in Sections 2.1 and 2.2, and we derive analytical expressions and carry out linear stability analysis for the coexistence equilibrium (i.e., where all three species coexist at nonzero densities) in each of the two smooth models. We are interested in the coexistence steady states because the data that we use in this work exhibit coexistence of predators and multiple prey. In Section 3, we discuss and use an existing data set for adaptively feeding plankton predators to fit model parameters and compare biomass predictions of the two smooth models. We summarize and discuss similarities and differences in model behavior and model assumptions between the piecewise-smooth system (analyzed in [35]) and its two smooth analogs (analyzed in this paper) in Section 4, and we conclude our study in Section 5. We give additional details about our calculations and analysis in a trio of appendices.

2 The models

We construct two smooth analogs of a piecewise-smooth model describing a predator population z that can adjust the extent of its consumption of its preferred prey p_1. The predator switches to consume only an alternative prey p_2 when predator fitness is maximized by doing so. To describe this situation, Ref. [35] developed the following piecewise-smooth dynamical system:

$$\dot{\mathbf{x}} = \begin{bmatrix} \dot{p_1} \\ \dot{p_2} \\ \dot{z} \end{bmatrix} = \begin{cases} f_+ = \begin{bmatrix} (r_1 - \beta_1 z)p_1 \\ r_2 p_2 \\ (eq_1\beta_1 p_1 - m)z \end{bmatrix} & \text{if } h = \beta_1 p_1 - a_q \beta_2 p_2 > 0 \\ f_- = \begin{bmatrix} r_1 p_1 \\ (r_2 - \beta_2 z)p_2 \\ (eq_2\beta_2 p_2 - m)z \end{bmatrix} & \text{if } h = \beta_1 p_1 - a_q \beta_2 p_2 < 0 \end{cases}, \tag{2.1}$$

where r_1 and r_2 (with $r_1 > r_2 > 0$) are the respective per capita growth rates of the preferred and alternative prey, $e > 0$ is the proportion of predation that goes into predator growth, β_1 and β_2 are the respective death rates of the preferred and alternative prey due to predation, q_1 and q_2 are nondimensional parameters that represent the predator's respective desire to consume the preferred and alternative prey, and $m > 0$ is the predator per capita death rate per day. In our construction of two smooth analogs of (2.1) and to facilitate our comparison between the piecewise-smooth and smooth systems, we take $\beta_1 = \beta_2 = 1$ for simplicity. The parameter a_q corresponds mathematically to the slope of the tilted switching manifold $h = \beta_1 p_1 - a_q \beta_2 p_2 = 0$ between the two vector fields in (2.1). Biologically, a_q is the slope of the assumed linear tradeoff in the predator's preference for prey. See [35] for biological justification of these model assumptions, analysis of the model (2.1), and inferred parameter values.

In the present paper, we construct and carry out linear stability analysis of two novel (to our knowledge) smooth models for an adaptively feeding predator and its two prey. First, we formulate the model in (2.1) as a three-dimensional smooth dynamical system with hyperbolic tangent functions in Section 2.1. Second, in Section 2.2, we construct a four-dimensional smooth analog of (2.1) by considering the desire to consume the preferred prey q_1 that changes between 1 and 0 across the discontinuity in the piecewise-smooth system (2.1) as a system variable that changes along with the population dynamics. We note that a subset of us incorporate a time-scale difference between demographic and trait (i.e., q_1) dynamics of the four-dimensional smooth analog and analyze it using singular perturbation theory in [36].

2.1 Smooth model I

Using a hyperbolic tangent as a transition function, we obtain the following smooth analog of (2.1):

$$\begin{aligned}
\dot{p_1} &= (r_1 - \beta_1 z)p_1 \left(\frac{1+\tanh(k(\beta_1 p_1 - a_q\beta_2 p_2))}{2}\right) \\
&\quad + r_1 p_1 \left(\frac{1-\tanh(k(\beta_1 p_1 - a_q\beta_2 p_2))}{2}\right) \equiv f(p_1,p_2,z)\,, \\
\dot{p_2} &= r_2 p_2 \left(\frac{1+\tanh(k(\beta_1 p_1 - a_q\beta_2 p_2))}{2}\right) \\
&\quad + (r_2 - \beta_2 z)p_2 \left(\frac{1-\tanh(k(\beta_1 p_1 - a_q\beta_2 p_2))}{2}\right) \equiv g(p_1,p_2,z)\,, \\
\dot{z} &= (eq_1\beta_1 p_1 - m)z \left(\frac{1+\tanh(k(\beta_1 p_1 - a_q\beta_2 p_2))}{2}\right) \\
&\quad + (eq_2\beta_2 p_2 - m)z \left(\frac{1-\tanh(k(\beta_1 p_1 - a_q\beta_2 p_2))}{2}\right) \equiv h(p_1,p_2,z)\,,
\end{aligned} \tag{2.2}$$

where k determines the steepness of the transition function and thus of switches in the predator's feeding behavior. In Section 3.1, we will infer values of k that best fit the data from a particular freshwater plankton system. The data were collected in Lake Constance between 1979 and 1999, were originally reported in [45,46], and were subsequently analyzed further in several papers (e.g., [47,48]). See Section 3 for a description of the data.

2.1.1 Linear stability analysis of smooth model I

In the Lake Constance data, several types of prey and predators coexist (see, e.g., [48]). We are therefore interested in a steady state of (2.2) with $p_1, p_2, z > 0$. We calculate

$$\begin{aligned}
f &= p_1\left(r_1 - z\left(\frac{1+\tanh(k(p_1 - a_q p_2))}{2}\right)\right) = 0 \\
&\Rightarrow z\left(\frac{1+\tanh(k(p_1 - a_q p_2))}{2}\right) = r_1
\end{aligned} \tag{2.3}$$

and

$$\begin{aligned}
g &= p_2\left(r_2 - z\left(\frac{1-\tanh(k(p_1 - a_q p_2))}{2}\right)\right) = 0 \\
&\Rightarrow z\left(\frac{1-\tanh(k(p_1 - a_q p_2))}{2}\right) = r_2\,,
\end{aligned} \tag{2.4}$$

so that

$$h = (eq_1\tilde{p}_1 - m)r_1 + (eq_2\tilde{p}_2 - m)r_2 = 0\,. \tag{2.5}$$

We obtain the steady-state solution $(\tilde{p}_1, \tilde{p}_2, \tilde{z})$, where

$$\begin{aligned}
\tilde{z} &= r_1 + r_2 \\
(eq_1\tilde{p}_1 - m)r_1 + (eq_2\tilde{p}_2 - m)r_2 &= 0 \\
\tanh(k(\tilde{p}_1 - a_q\tilde{p}_2)) &= \frac{r_1 - r_2}{r_1 + r_2}\,.
\end{aligned} \tag{2.6}$$

Taking the inverse hyperbolic tangent on both sides of the third equation in (2.6) results in linear independent equations for $\tilde{p}_1$ and $\tilde{p}_2$. There thus exists a unique coexistence steady state at

$$\begin{aligned}
\tilde{p}_1 &= \frac{a_q m(r_1+r_2) + \frac{eq_2 r_2 \operatorname{arctanh}\left(\frac{r_1-r_2}{r_1+r_2}\right)}{k}}{e(q_1 a_q r_1 + q_2 r_2)}\,, \\
\tilde{p}_2 &= \frac{m(r_1+r_2) - \frac{eq_1 r_1 \operatorname{arctanh}\left(\frac{r_1-r_2}{r_1+r_2}\right)}{k}}{e(q_1 a_q r_1 + q_2 r_2)}\,, \\
\tilde{z} &= r_1 + r_2\,.
\end{aligned} \tag{2.7}$$

All three population densities are positive at the steady state $(\tilde{p}_1, \tilde{p}_2, \tilde{z})$ when

$$k > k_0 = \frac{eq_1 r_1 \operatorname{arctanh}\left(\frac{r_1 - r_2}{r_1 + r_2}\right)}{m(r_1 + r_2)} \,. \tag{2.8}$$

We use the Routh–Hurwitz criterion [19, 38] to investigate the stability of the coexistence steady state (2.7).

Proposition 2.1. *If $a_q \geq q_2/q_1$, then the steady state (2.7) is stable if and only if $k > k_0$.*

Proof. See Appendix A. □

Proposition 2.2. *If $a_q < q_2/q_1$, then there exists $k_1 \in (k_0, \infty)$ so that the steady state (2.7) is stable if and only if $k \in (k_0, k_1)$.*

Proof. See Appendix A. □

Consequently, when a_q is large, which corresponds to a predator with a steep tradeoff in its prey preference (i.e., a small increase in specialization towards the preferred prey comes at a large cost of the growth obtained from feeding on the alternative prey), the coexistence steady state (2.7) is stable for all $k > k_0$. When the prey switching is steep (i.e., when $k \to \infty$), the coexistence steady state (2.7) is equal to the steady state of the piecewise-smooth system that lies on the switching manifold (i.e., it is a *pseudoequilibrium*), and it has a complex-conjugate pair of eigenvalues with negative real part when $a_q > q_2/q_1$ [35]. However, in contrast to the piecewise-smooth system, in which the coexistence steady state is repelling for shallow or flat prey preference tradeoffs (i.e., when $a_q < q_2/q_1$), the smooth system (2.2) has an interval of intermediate prey-switching slopes $k \in (k_0, k_1)$ (see Equation (A.9) for the expression for k_1) for which the coexistence state is also stable for $a_q < q_2/q_1$.

2.2 Smooth model II

To represent the three-dimensional piecewise-smooth system (2.1) as a four-dimensional smooth system, we construct expressions for the temporal evolution of the predator's trait to accompany the population dynamics of the predator and two prey. Biologically, we assume that the predator's desire to consume the preferred prey undergoes either *rapid evolution* [10] or *phenotypic plasticity* [26], which are the two forms of adaptivity in organisms. We will comment on these model assumptions in Section 4. We thereby represent the parameter q_1 that abruptly changes across the discontinuity in the piecewise-smooth model (2.1) (i.e., $q_1 = 1$ when $h > 0$ and $q_1 = 0$ when $h < 0$) as a system variable q that changes in response to the prey abundance on the same time scale as the population dynamics in a smooth dynamical system.

To ensure similarity with the piecewise-smooth model (2.1), we assume that a small preference towards the preferred prey amounts to a feeding mode of consuming only the alternative prey (i.e., $q = 0$) and that a large preference towards the preferred prey amounts to a feeding mode of consuming only the preferred prey (i.e., $q = 1$). We incorporate this assumption with a bounding function $q(1-q)$ in the expression for the temporal evolution of the predator's trait. From the condition for prey switching derived using optimal foraging theory [42] in [35], we impose that the rate of change of the mean trait value is proportional to $p_1 - a_q p_2$. In other words, we assume that the predator's choice to switch prey depends on prey abundances and which diet composition maximizes the predator's rate of energy intake [42]. In addition, we assume exponential prey growth and linear functional response as in the piecewise-smooth system in (2.1) [35], and there we obtain the following dynamical system for the population dynamics coupled with the temporal evolution of the predator trait:

$$\begin{aligned}
\frac{\mathrm{d}p_1}{\mathrm{d}t} &= \dot{p_1} = g_1(p_1, p_2, z, q) = r_1 p_1 - q p_1 z \,, \\
\frac{\mathrm{d}p_2}{\mathrm{d}t} &= \dot{p_2} = g_2(p_1, p_2, z, q) = r_2 p_2 - (1-q) p_2 z \,, \\
\frac{\mathrm{d}z}{\mathrm{d}t} &= \dot{z} = g_3(p_1, p_2, z, q) = eq p_1 z + e(1-q) q_2 p_2 z - m z \,, \\
\frac{\mathrm{d}q}{\mathrm{d}t} &= \dot{q} = f(p_1, p_2, q) = q(1-q)(p_1 - a_q p_2) \,.
\end{aligned} \tag{2.9}$$

As a result of our similar model assumptions, the smooth model (2.9) reduces to f_+ in (2.1) when $q = 1$ and to f_- in (2.1) when $q = 0$. Biologically, these two cases correspond, respectively, to the situations in which the predator's diet is composed solely of the preferred and alternative prey type.

2.3 Linear stability analysis of smooth model II

The population densities of the predator and two prey types at the coexistence steady state in the second smooth system (2.9) are

$$\begin{aligned} \tilde{p}_1 &= \frac{a_q m(r_1 + r_2)}{e(r_1 a_q + r_2 q_2)}\,, \\ \tilde{p}_2 &= \frac{m(r_1 + r_2)}{e(r_1 a_q + r_2 q_2)}\,, \\ \tilde{z} &= r_1 + r_2\,, \\ \tilde{q} &= \frac{r_1}{r_1 + r_2}\,. \end{aligned} \tag{2.10}$$

These are the same densities that occur at the pseudoequilibrium point of the piecewise-smooth system (2.1) (for $q_1 = 1$) that is located on the discontinuity boundary of the piecewise-smooth 1 predator–2 prey model [35]. We summarize the result of linear stability analysis of the smooth system (2.9) in the two following propositions.

Proposition 2.3. *If $a_q = q_2$, then all eigenvalues of the steady state are purely imaginary.*

Proof. See Appendix B. □

Proposition 2.4. *If $a_q \neq q_2$, then the steady state is linearly unstable.*

Proof. See Appendix B. □

Consequently, the smooth system (2.9) exhibits an unstable coexistence steady state irrespective of whether a predator species can be construed as a selective predator with a steep preference tradeoff with respect to its preferred and alternate prey or as an unselective predator species with a mild tradeoff in its preference towards the two prey. Our results also imply that our smoothing the piecewise-smooth system (2.1) by adding an extra dimension as in Equation (2.9) changes the stability of the coexistence equilibrium.

3 Comparison of model simulations and Lake Constance data

We now compare model simulations with data (which were reported first in [45] and later in [47]) for *ciliate* predators and two different types of their algal prey collected from Lake Constance on the German–Swiss–Austrian border. Ciliates are eukaryotic single cells that propel using small protuberances (i.e., *cilia*) that project from their cell body. They occur in aquatic environments and constitute an important link between the primary producers and higher levels of aquatic food webs [47]. The Lake Constance data set consists of over 23,000 observations of abundances (individuals or cells per milliliter) and biomass (units of carbon per square meter) of various plankton species obtained at least once in a sample of a few milliliter to a liter of water between March 1979 and December 1999 [45, 47]. We compare the abundances predicted by our two smooth models with data from years 1991 and 1998. (For a comparison between the piecewise-smooth model (2.1) and data, see [35].) During these two years, the spring bloom lasted for several weeks, and ciliate and algal biomasses exhibited recurring patterns of increases followed by declines [46]. We are interested in spring abundances because previous studies suggested that predator–prey feeding interactions are an important factor in explaining the ciliate–algae dynamics in that season [48] and such interactions are more important than environmental conditions during spring [40].

Müller and Schlegel observed ciliates actively selecting against certain types of prey when offered a mixed diet of different types of their algal prey [33]. It has been suggested by Müller and Schlegel that adaptive feeding in ciliates occurs because different species benefit differently depending on the match between their feeding mode and the prey species that are abundant in the prey community. That is, ciliates select against their less edible prey (e.g., a prey type that develops a hard silicate cover as a predator defense mechanism) when offered a mixed diet of both easily digested and less edible prey [33]. The piecewise-smooth dynamical system (2.1) reproduces patterns that are exhibited by the Lake Constance data and suggests that prey switching in the presence of a preference tradeoff is a possible mechanistic explanation of the observed dynamics [35]. Moreover, one can categorize ciliates, which dominate the herbivorous zooplankton community in spring [46], roughly in terms of being more or less selective predators [52]. To represent differences in selectivity between different predator species, we consider a "filter feeder" ciliate species that sieves suspended food particles as an example of a less selective predator. For a more selective predator, we use an "interception feeder" ciliate species that scavenges food particles and intercepts them directly.

For our comparison between the Lake Constance data and the two smooth models in Sections 3.1 and 3.2, we first normalize both the biweekly data points and the model predictions for the predator density z by the L_2-norm (i.e., the Euclidean distance). We consider the time window from 1 March to 15 June, for which there are 31 data points for the selective predator and 19 data points for the unselective predator in 1991. In 1998, there are 15 data points for both the selective and unselective predator species between 1 March and 15 June. To do our parameter fitting, we use approximate Bayesian computation (ABC) combined with a population Monte Carlo (PMC) method [3], because it allows one to study the results from the posterior parameter distribution. This is especially useful for assessing how well the piecewise-smooth model (2.1) approximates prey switching, which we represent with a hyperbolic tangent function in one smooth model (2.2) and by incorporating an additional system variable in the other smooth model (2.9).

3.1 Smooth model I simulations and data

In this section, we fit the growth rates of the preferred and alternative prey (r_1 and r_2, respectively), the predator mortality rate m, the slope k of the prey-switching function, and the slope a_q of the prey-preference tradeoff of the smooth model (2.2). We use a_q as a bifurcation parameter. (See Propositions 2.1 and 2.2.)

The smooth model (2.2) reproduces the peak abundances in the Lake Constance data and predicts an oscillatory pattern for both the selective and unselective predator populations during the springs of 1991 and 1998 (see Figures 1 and 2). Additionally, parameter fitting suggests that adaptive feeding of the selective predator is best represented with a steep switching function. In particular for year 1998, we obtain a higher frequency of small k for an unselective predator than for a selective one at the smallest tolerance level of the fitting algorithm. See the middle rows of Figures 1 and 2. However, the coexistence steady state is unstable for the parameter values that we use in the top right panels in Figures 1 and 2. In these two figures, this steady state is thus unstable for $k > k_1 \approx 1.3$ and $k > k_1 \approx 2.9$, respectively.

Simulations of the smooth model (2.2) with parameter values, which we obtain by fitting the model to the selective predator data in year 1998, predict that the amplitude of the oscillations in the preferred prey population are smaller than the amplitude of the oscillations in the alternative prey population. As we illustrate in Figure 3, this is different from the Lake Constance data for the two prey groups in the same year 1998. However, similarly to the case of the predator population, the first smooth model is able to capture the timing of the peak densities of the prey populations, although the prey data is not used to fit the model parameters (see Figure 3).

3.2 Smooth model II simulations and data

To compare simulations of the smooth model (2.9) to data, we fit the prey growth rates r_1 and r_2, the predator mortality rate m, and a perturbation ν in the predator population from the coexistence steady state in Equation (2.10) for $a_q = q_2 = 0.5$ (i.e., all four eigenvalues of the coexistence steady state are purely imaginary). We thus use $(p_1(0), p_2(0), z(0), q(0)) = (a_q m(r_1 + r_2)/[e(r_1 a_q + r_2 q_2)], m(r_1 + r_2)/[e(r_1 a_q + r_2 q_2)], \nu(r_1 + r_2), r_1/(r_1 + r_2))$ as our initial value for the model simulations to infer values for ν that minimize the distance in Equation (C.1) between the data points and the model prediction for these points.

As in the case of the first smooth model I, the second smooth model reproduces the peak predator

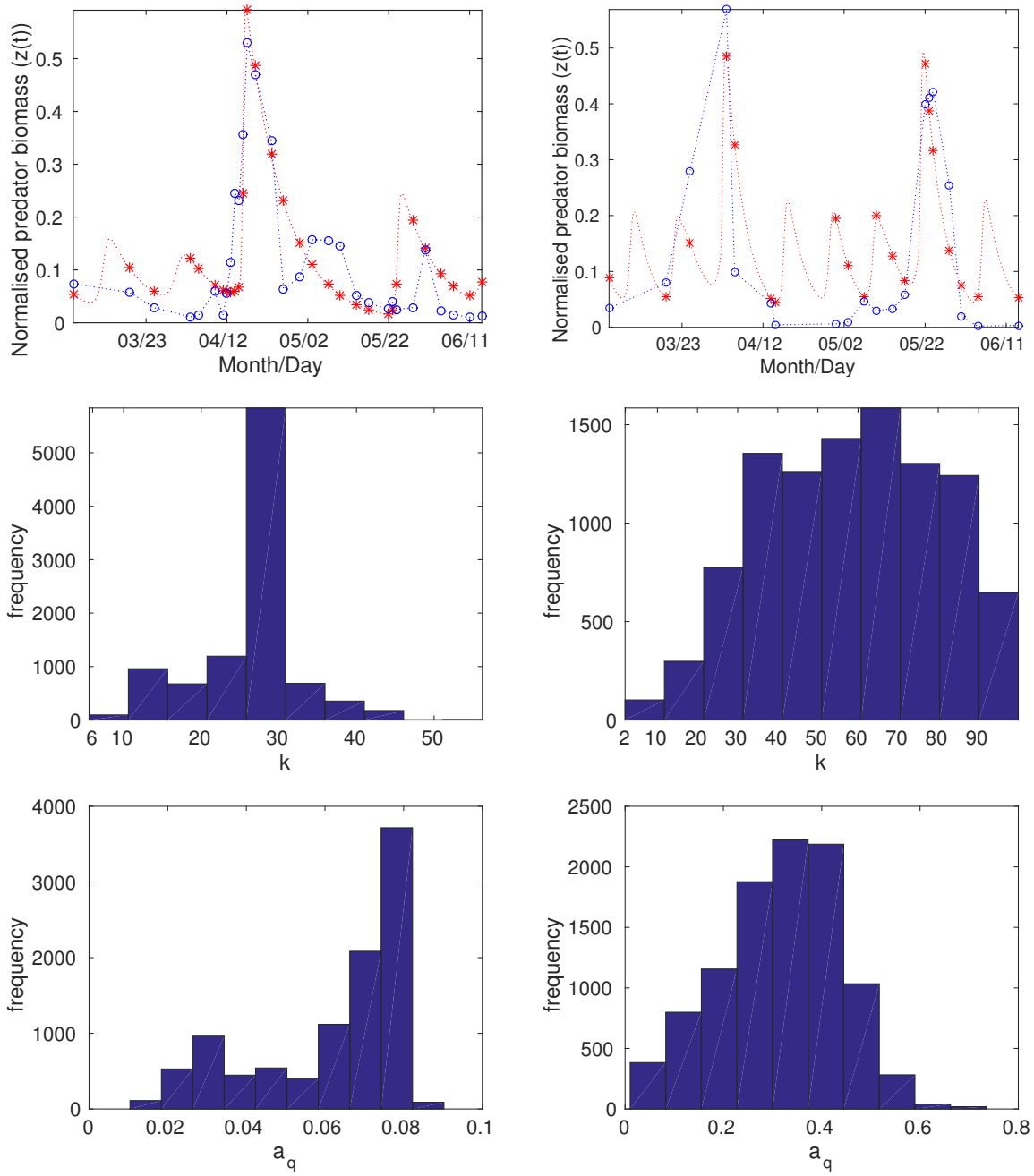

Figure 1: (Top panels) The red asterisks give the normalized predator abundance $z(t)$ for simulations of (2.2) using the parameter values $q_1 = 1$, $q_2 = 0.5$, $e = 0.25$, and $\beta_1 = \beta_2 = 1$ and fitted values of (left) $r_1 \approx 1.64$, $r_2 \approx 0.62$, $m \approx 0.11$, $a_q \approx 0.02$, and $k \approx 31$ and (right) $r_1 \approx 2.54$, $r_2 \approx 0.61$, $m \approx 0.21$, $a_q \approx 0.04$, and $k \approx 67$. To guide the eye, we show the simulation in red between the asterisks. We show the normalized data using blue circles, and we show blue lines between them to guide the eye. We also show bar plots for the frequency of (center panels) k values and (bottom panels) a_q values at the strictest tolerance level ($Tol_{10} \approx 0.00789$ in the left panels and $Tol_{15} \approx 0.0258$ in the right panels) using the PMC ABC method [3] for (left) selective and (right) unselective predator groups in spring in Lake Constance in 1991. Each frequency plot represents a random weighted sample (of size 10000) from the parameter values accepted at the strictest tolerance level. The squared distance [see Equation (C.1)] between the asterisks (model prediction) and circles (data) is (left) 0.0094 and (right) 0.0102. For more details of the parameter fitting, see Appendix C. The unselective predator group consists of data for *Rimostrombidum lacustris*, and the selective predator group consists of data for *Balanion planctonicum*.

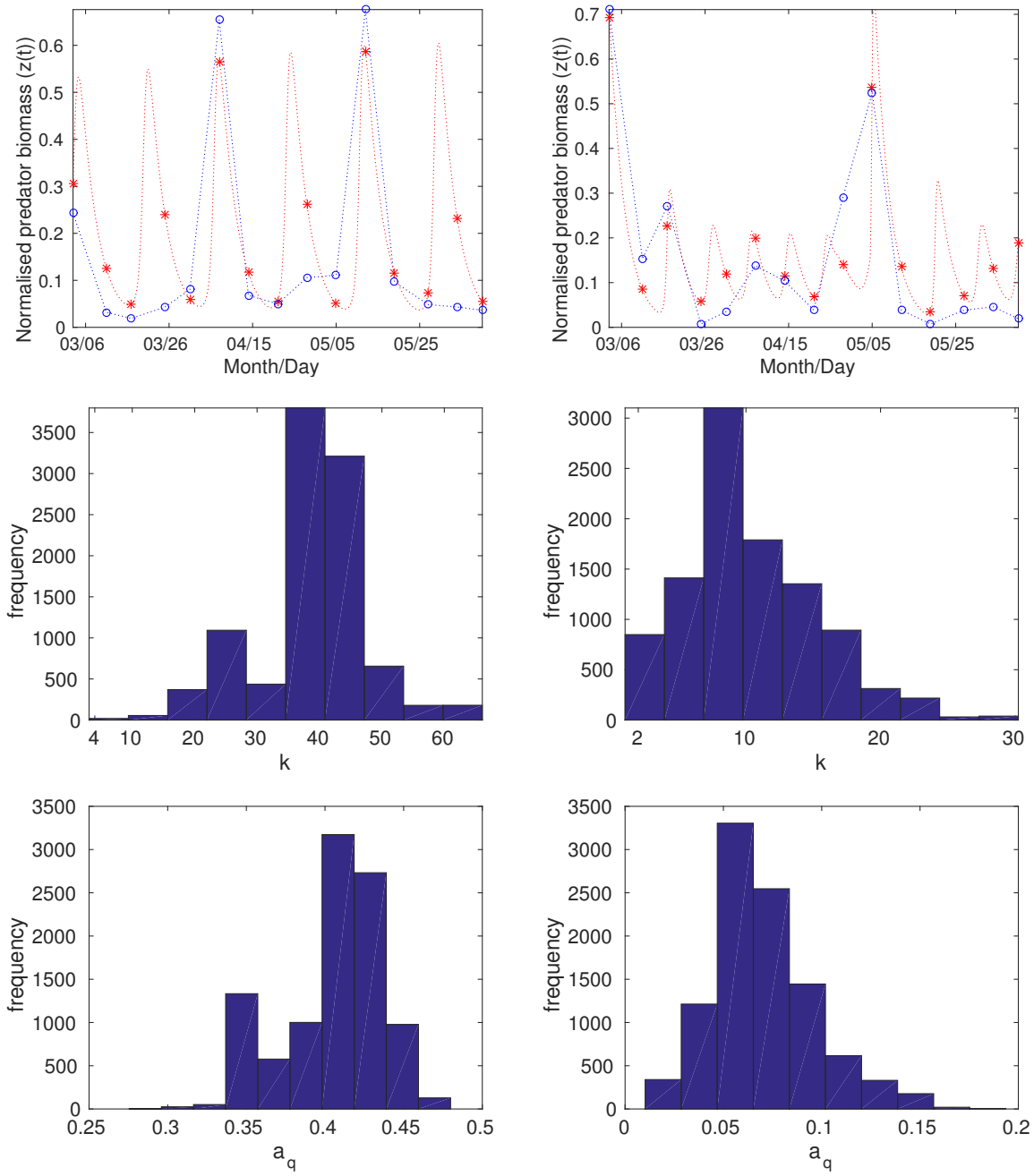

Figure 2: (Top panels) The red asterisks give the normalized predator abundance $z(t)$ for simulations of (2.2) for parameter values $e = 0.25$ and $\beta_1 = \beta_2 = 1$ and fitted values (left) $r_1 \approx 1.12$, $r_2 \approx 0.76$, $m \approx 0.25$, $a_q \approx 0.42$, and $k \approx 38$ and (right) $r_1 \approx 2.32$, $r_2 \approx 0.51$, $m \approx 0.27$, $a_q \approx 0.027$, and $k \approx 16$. To guide the eye, we show the simulation in red between the asterisks. We show the normalized data using blue circles, and we show blue lines between them to guide the eye. We also show bar plots for the frequency of (center panels) k values and (bottom panels) a_q values at the strictest tolerance level ($Tol_{15} \approx 0.0213$ in the left panels and $Tol_{15} \approx 0.0229$ in the right panels) using the PMC ABC method [3] for (left) selective and (right) unselective predator groups in spring in Lake Constance in 1998. Each frequency plot represents a random weighted sample (of size 10000) from the parameter values accepted at the strictest tolerance level. The squared distance [see Equation (C.1)] between the asterisks (model prediction) and circles (data) is (left) 0.0090 and (right) 0.0061. For more details of the parameter fitting, see Appendix C. The unselective predator group consists of data for *Rimostrombidum lacustris*, and the selective predator group consists of data for *Balanion planctonicum*.

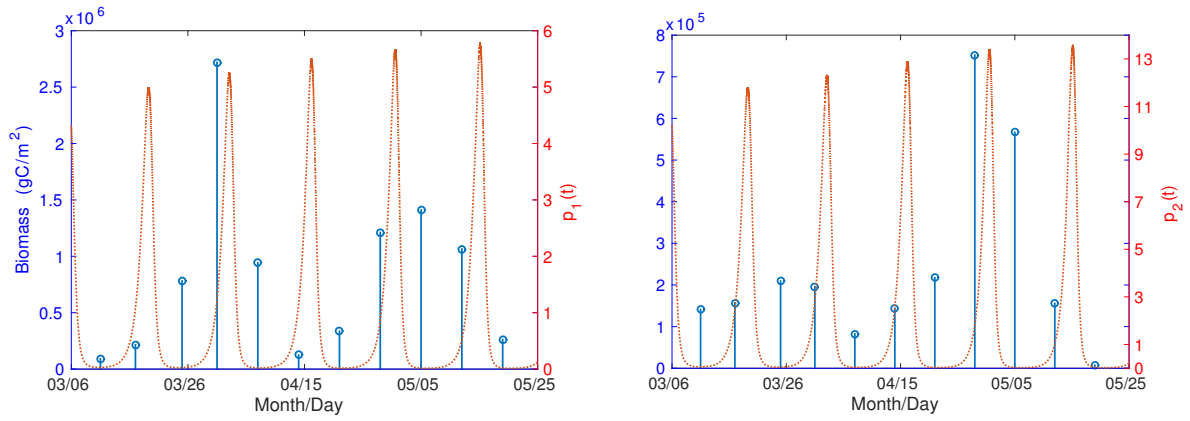

Figure 3: (Left, red) Preferred prey abundance $p_1(t)$ and (right, red) alternative prey abundance $p_2(t)$ for simulations of (2.9) using the same parameter values as in the left panel of Figure 2. (Left, circles) preferred and (right, circles) alternative prey data in spring in Lake Constance in 1998. The preferred prey group consists of data for *Cryptomonas ovata*, *Cryptomonas marssonii*, *Cryptomonas reflexa*, *Cryptomonas erosa*, *Rhodomonas lens*, and *Rhodomonas minuta*. The alternative prey group consists of data for small and medium-size *Chlamydomonas* spp. and *Stephanodiscus parvus*.

densities and thereby suggests that a large perturbation from the coexistence steady state does a good job at fitting the second smooth model to the data. See Figures 4 and 5. For year 1991, we predict that the selective predator group switches its diet less frequently than the unselective predator. Additionally, $q(t)$ reaches its maximum and minimum values. In contrast, for the unselective predator, there is a change from increasing to decreasing in $q(t)$ at an intermediate value. See figures for $q(t)$ at the bottom of the top panels of Figures 4 and 5. We predict that the switching of the selective predator occurs more often in year 1998 than in year 1991 (and in 1998, it occurs also more often than that of the unselective predator) (see Figure 5).

Our model prediction for prey abundances suggests for an unselective predator in year 1991 that the preferred prey has smaller-amplitude oscillations than the alternative prey. As we show in Figure 6, this differs from the data. We note that this is the case with the first smooth model(2.2) as well (see Figure 3). Nevertheless, although we only use predator data to fit parameters, the second smooth model (2.9) is also able to successfully capture some features of the prey data. As we illustrate in the left panel of Figure 6, such features include the periodicity of the peak densities of the preferred prey populations.

4 Discussion

Our first smooth system (2.2) necessitates the incorporation of a parameter k that influences the system's qualitative behavior, whereas our second smooth system (2.9) has the same number of parameters as the piecewise-smooth system (2.1) but has an additional system variable. Consequently, it can be advantageous to study the piecewise-smooth system, especially if many species are included, because it allows one to avoid adding new parameters and/or variables. The hyperbolic tangent functions in (2.2) and the increased dimensionality of (2.9) both add complications to analytical calculations and parameter fitting. On the bright side, both standard numerical techniques and standard theory to determine the stability of equilibria using linear stability analysis and study bifurcations are best developed for smooth dynamical systems. In contrast, one needs to use more involved methods for theory and numerical computations for piecewise-smooth dynamical systems, and development of these techniques is an active area of research [8]. However, one can derive an analytical expression for the flow at the discontinuity boundary (i.e., $h = \beta_1 p_1 - a_q \beta_2 p_2 = 0$) of (2.1), and the available theory for piecewise-smooth dynamical systems identifies the bifurcation that takes place in (2.1) as a_q crosses the value $a_q = q_2/q_1$ [35]. These results help facilitate understanding of the behavior of (2.1) that can be used when analyzing the ciliate–algae dynamics predicted by the piecewise-smooth model [35].

From a biological perspective, using a smooth dynamical system allows us to relax the assumption of a "discontinuous" predator of the piecewise-smooth system (2.1). When the discontinuity is smoothed out using hyperbolic tangent functions, as in (2.2), we can use data to determine the steepness of the transition in the predator's feeding behavior for a particular predator type. Indeed, our parameter

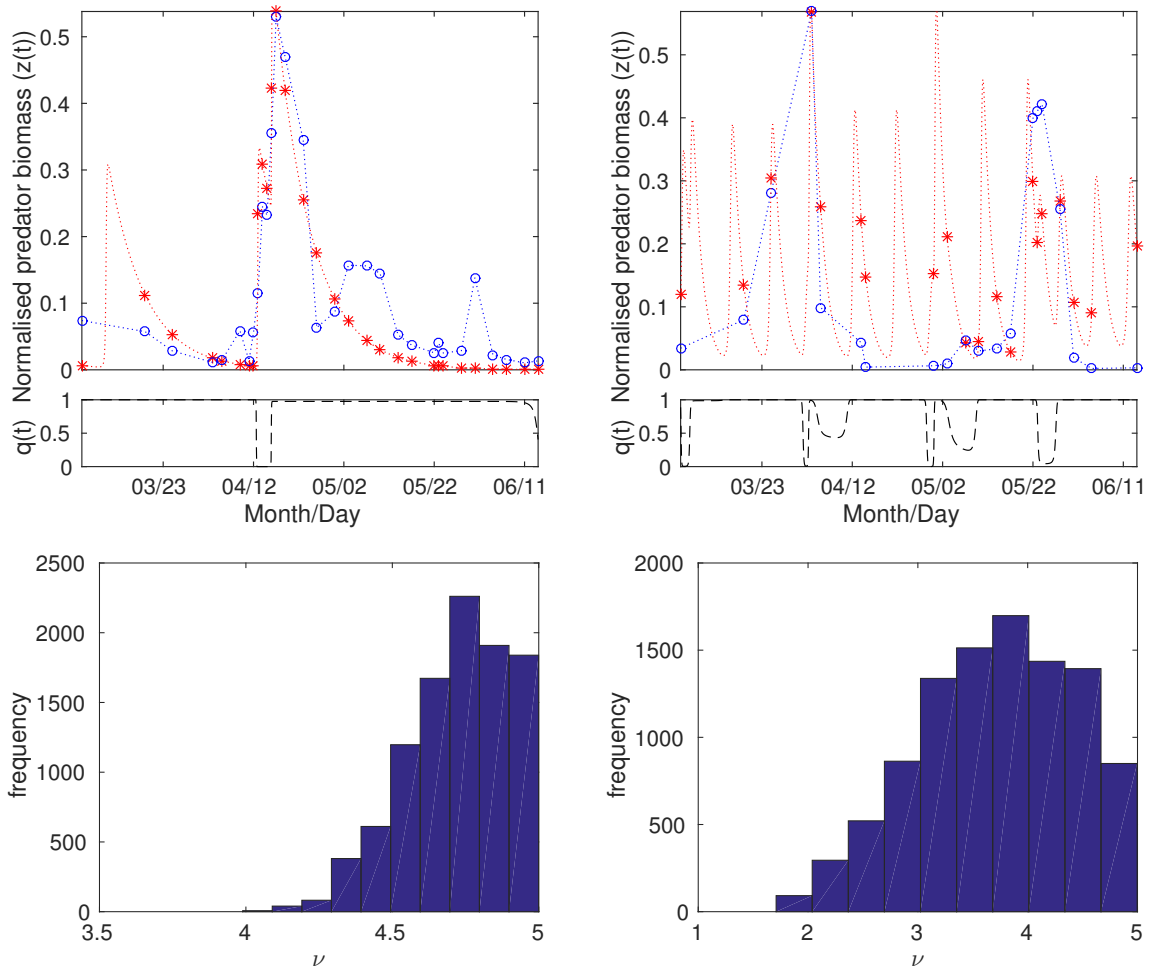

Figure 4: (Top panels) The red asterisks give the normalized predator abundance $z(t)$ for simulations of (2.9) with an initial value of $z(0) = \nu(r_1 + r_2)$, the steady-state densities in (2.10), parameter values of $e = 0.25$, $\beta_1 = \beta_2 = 1$, and $a_q = q_2 = 0.5$, and fitted values of (left) $r_1 \approx 3.00$, $r_2 \approx 0.62$, $m \approx 0.12$, and $\nu \approx 4.8$ and (right) $r_1 \approx 2.21$, $r_2 \approx 0.33$, $m \approx 0.48$, and $\nu \approx 4.6$. To guide the eye, we show the simulation in red between the asterisks. We show the normalized data using blue circles, and we plot blue lines between them to guide the eye. (Bottom panels) We show bar plots for the frequency of ν values at the strictest tolerance level ($\text{Tol}_{10} \approx 0.00815$ in the left panel and $\text{Tol}_{13} \approx 0.0233$ in the right panel) using the PMC ABC method [3] for (left) selective and (right) unselective predator groups in spring in Lake Constance in 1991. Each frequency plot represents a random weighted sample (of size 10000) from the parameter values at the strictest tolerance level. The squared distance [see Equation (C.1)] between the asterisks (model prediction) and circles (data) is (left) 0.0038 and (right) 0.0151. For more details of the parameter fitting, see Appendix C. The unselective predator group consists of data for *Rimostrombidum lacustris*, and the selective predator group consists of data for *Balanion planctonicum*.

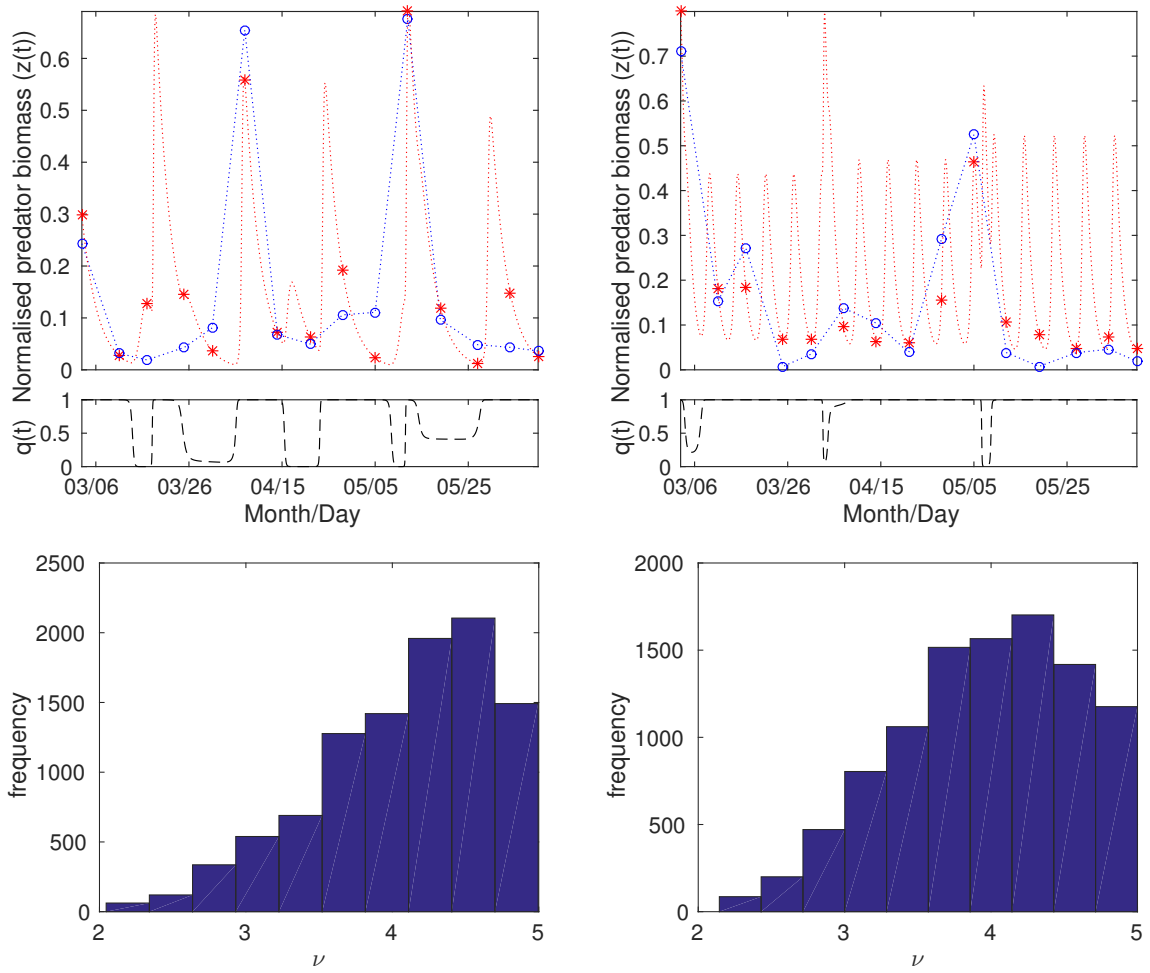

Figure 5: (Top panels) The red asterisks give the normalized predator abundance $z(t)$ for simulations of (2.9) with an initial value of $z(0) = \nu(r_1 + r_2)$, the steady-state densities in (2.10), parameter values of $e = 0.25$, $\beta_1 = \beta_2 = 1$, and $a_q = q_2 = 0.5$, and fitted values of (left) $r_1 \approx 1.62$, $r_2 \approx 0.40$, $m \approx 0.30$, and $\nu \approx 4.8$ and (right) $r_1 \approx 1.95$, $r_2 \approx 0.24$, $m \approx 0.72$, and $\nu \approx 3.58$. To guide the eye, we show the simulation in red between the asterisks. We show the normalized data using blue circles, and we plot blue lines between them to guide the eye. (Bottom panels) We show bar plots for the frequency of ν values at the strictest tolerance level ($\text{Tol}_{13} \approx 0.0245$ in the left panel and $\text{Tol}_{13} \approx 0.0231$ in the right panel) using the PMC ABC method [3] for (left) selective and (right) unselective predator groups in spring in Lake Constance in 1998. Each frequency plot represents a random weighted sample (of size 10000) from the parameter values at the strictest tolerance level. The squared distance [see Equation (C.1)] between the asterisks (model prediction) and circles (data) is (left) 0.0043 and (right) 0.0039. For more details of the parameter fitting, see Appendix C. The unselective predator group consists of data for *Rimostrombidum lacustris*, and the selective predator group consists of data for *Balanion planctonicum*.

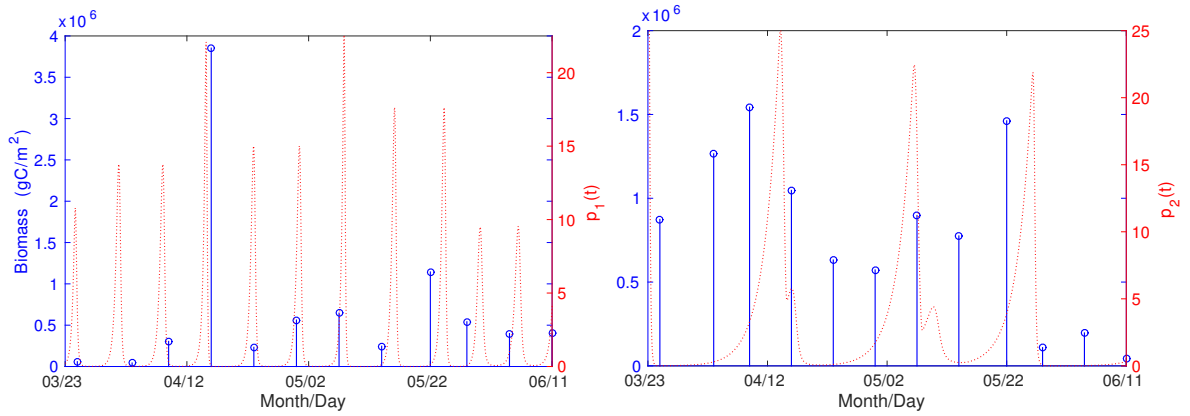

Figure 6: (Left, red) Preferred prey abundance $p_1(t)$ and (right, red) alternative prey abundance $p_2(t)$ for simulations of (2.9) using the same parameter values as in the right panel of Figure 4. (Left, circles) preferred and (right, circles) alternative prey data in spring in Lake Constance in 1991. The preferred prey group consists of data for *Cryptomonas ovata*, *Cryptomonas marssonii*, *Cryptomonas reflexa*, *Cryptomonas erosa*, *Rhodomonas lens*, and *Rhodomonas minuta*. The alternative prey group consists of data for small and medium-size *Chlamydomonas* spp. and *Stephanodiscus parvus*.

fitting to the Lake Constance data suggests that one can model prey switching in either a selective and an unselective predator species using a steep hyperbolic tangent function. Additionally, our parameter fitting of the first smooth model (2.2) predicts that the best fit to the data occurs in the parameter regime in which the coexistence steady state is unstable. For the second smooth system (2.9), which regularizes the abrupt change in the predator's diet choice by considering a predator trait as a system variable, we obtain a model prediction for predator trait dynamics, i.e., for the temporal evolution of the predator's desire to consume the preferred prey p_1.

Parameter fitting to Lake Constance data suggests that the best fit occurs in a parameter regime in which the predator trait dynamics oscillate abruptly between the maximum and minimum values. In a study of two plankton predators and their evolving algal prey, Hiltunen et al. show and discuss experimental evidence for periods of dominance of one predator followed by a rapid switch to a dominance by the other [14]. In [14], the switch in the predator dominance can be explained by the interaction between changes in the predator population and those in the frequency of the prey type that develops a predator defense mechanism against one of the two predators. Motivated by the above findings, it is also interesting to consider a model in which one incorporates a time-scale difference between demographic and predator trait dynamics [36]. In our ongoing work, we aim to increase the current understanding of differences and similarities between piecewise-smooth, smooth, and fast-slow dynamical systems by comparing the behavior of these different models both qualitatively and quantitatively to each other. For example, one possible avenue for future work is to test our model predictions for prey death rates to results from controlled laboratory experiments with genetically diverse prey and/or predator populations in which one can record the dynamics of the genetic diversity. Such trait dynamics cannot be obtained from either the piecewise-smooth dynamical system (2.1) or our first smooth system (2.2), but they can be examined in our second smooth model (2.9) (and in the fast-slow system analyzed in [36]).

Both of our smooth models successfully reproduce the peak population densities and suggest that a parameter regime — when $a_q < q_2/q_1$ for the first smooth model (2.2) and for a large perturbation from the steady state for the second smooth model (2.9) — fits the data for ciliate predators in Lake Constance in the springs of 1991 and 1998. Additionally, when using the parameters that we obtain from fitting the second smooth model to data for the unselective predator in year 1991, we obtain agreement between our model's prediction and the periodicity of the peak prey abundances. A good fit at peak abundances is somewhat expected, because we introduce a phase shift in the model prediction before calculating the distance between the prediction and the data. (In other words, we align the maximum in the model prediction with the maximum in the data.) Such a procedure results in several candidate parameter sets to be rejected (e.g., because they predict a steady state); this increases computation time. An alternative to using a phase shift is to fit the initial values simultaneously with the model parameters. In such an approach, one can compare the distances between the periodic orbits predicted by the model to those exhibited in the data. However, it is not clear how one should choose a reasonable time window for fitting the initial values and whether such a modification would yield more effective parameter fitting

than with the current approach.

Both of our smooth models predict a higher frequency of peak densities than what we observe in the available data points. A high period in population oscillations is possible for small organisms, such as plankton, with short lifespans and large population densities. However, making measurements more frequent than biweekly would be a good way to try to validate or discard the periodicity predicted by the smooth models. Additionally, using data comparison to choose between different competing models would be an effective way to help increase current understanding of the use of a piecewise-smooth model as a simplification of a steep transition in plankton-feeding behavior. Such comparisons would also be valuable more generally in numerous applications. In practice, one can implement such a model comparison using a heuristic method (e.g., approximate Bayesian computation, as in the present paper) [49] or by using existing toolboxes for system identification (e.g., implemented in MATLAB [20]).

From a modeling perspective, the piecewise-smooth system (2.1) incorporates the effects of a predator's adaptive change of diet in response to prey abundance, whereas the second smooth system (2.9) (with an appropriate choice of parameters) recovers a model for rapid evolutionary change in the predator's desire to consume its preferred prey [36]. Consequently, the second smooth system models a different mechanism (*rapid evolution* [10]) than the piecewise-smooth system (*phenotypic plasticity* [26]) for how rapid adaptation affects population dynamics [39, 53]. It has been suggested that a stable equilibrium can be more expected from models that account for phenotypic plasticity than from those that account for rapid evolution, because plastic genotypes respond faster than nonplastic genotypes to fluctuating environmental conditions [53]. Our modeling work is consistent with this hypothesis, as the piecewise-smooth system (2.1) converges to a steady state for a large region of space [35], but the same steady state is unstable (except for one point ($a_q = q_2$) at which it is nonhyperbolic) in the second smooth system (2.9).

5 Conclusions

To relax the simplifying assumption of a discontinuity in a model for a predator adaptively feeding on two different types of prey, we constructed two regularizations of a piecewise-smooth dynamical system (2.1). In one model, we smoothed out the transitions using the hyperbolic tangent function; in the other, we added a new system variable to the system (and hence increased the system dimension by 1). Similar to earlier studies, such as [21, 31], our study provides an illustrative example of both similarities and differences between a piecewise-smooth system and smooth analogs to it. For example, although the population densities at a coexistence equilibrium are the same in all three models (when $k \to \infty$), adding a dimension to the system destabilizes the equilibrium. Moreover, although the two smooth analogs agree with the piecewise-smooth system in the appropriate limiting cases (i.e., when $k \to \infty$ and when $q = 0/q = 1$), the smooth system with hyperbolic tangent functions converges to an equilibrium for a gradual transition, whereas there is a periodic orbit in the corresponding piecewise-smooth system. When piecewise-smooth dynamical systems are used to simplify transitions in applications — such as approximating a cubic function in a membrane potential in models of spiking neurons [32], Hill functions in models of gene regulatory networks [12], or changes in the Earth's reflectivity due to ice melt in climate models [1] — understanding the extent to which the behavior of the corresponding smooth and piecewise-smooth systems agree is crucial for generating both an accurate model simplification and accurate model predictions.

Based on our results from fitting parameters of the two smooth systems to data on freshwater plankton, we conclude that the simplifying assumption of a discontinuous predator is justified. In our work, our use of a regularization that increases the dimensionality of the original piecewise-smooth system by 1 has also yielded a model prediction for the predator trait dynamics that can be validated, for example, with data describing the dominating trait value within the predator population. Such a comparison would help not only develop new biological understanding of the coupling between ecology and phenotypic plasticity, as we consider in the four-dimensional smooth model, but also determine if phenotypic plasticity is a possible mechanistic explanation for observed demographic and trait dynamics. Using the data that we currently possess, it is difficult to determine which of the three models (i.e., the piecewise-smooth system with a "discontinuous" predator or the two smooth systems with a gradually adapting predator) provides a better putative mechanistic explanation for the observations of ciliate–algae dynamics in spring in Lake Constance. In particular, data on the functional form of prey switching and on the periodicity of the population oscillations would be very useful for model selection. Nevertheless, the construction of models using alternative modeling approaches, transforming between them, and comparing them to data can

greatly increase understanding of the underlying mechanisms of complex systems. Such understanding can then can be used to improve the predictability of their models.

Acknowledgements

We thank John Hogan, Philip Maybank, Frits Veerman, and Frank Schilder for helpful discussions. We thank Ursula Gaedke for sending us the Lake Constance data, which were obtained as part of the Collaborative Programme SFB 248 funded by the German Science Foundation. SHP was supported by Osk. Huttunen Foundation (OHF) and Engineering and Physical Sciences Research Council (EPSRC) through the Oxford Life Sciences Interface Doctoral Training Centre and by People Programme (Marie Curie Actions) of the European Union's Seventh Framework Programme (FP7/2007-2013) under REA grant agreement #609405 (COFUNDPostdocDTU).

A Stability of the coexistence steady state in smooth model I

In this appendix, we prove Propositions 2.1 and 2.2.

Proof. The Jacobian of equation (2.2) is:

$$\begin{bmatrix} r_1 - \frac{z}{2}B\left(1+p_1kC\right) & \frac{zp_1ka_q}{2}BC & \frac{-p_1}{2}B \\ \frac{zp_2k}{2}BC & r_2 - \frac{z}{2}C\left(1+p_2ka_qB\right) & \frac{-p_2}{2}C \\ \frac{eq_1z}{2}B\left(1+p_1kC\right) - \frac{eq_2p_2zk}{2}BC & \frac{eq_2z}{2}C\left(1+p_2ka_qB\right) - \frac{eq_1p_1zka_q}{2}BC & \frac{eq_1p_1}{2}B + \frac{eq_2p_2}{2}C - m \end{bmatrix}, \tag{A.1}$$

where

$$\begin{aligned} A &= \tanh\left(k\left(p_1 - a_qp_2\right)\right), \\ B &= 1 + A, \\ C &= 1 - A. \end{aligned} \tag{A.2}$$

At the coexistence steady state (2.7), the Jacobian (A.1) reduces to

$$\frac{1}{r_1+r_2}\begin{bmatrix} -2r_1r_2k\tilde{p}_1 & 2r_1r_2ka_q\tilde{p}_1 & -r_1\tilde{p}_1 \\ 2r_1r_2k\tilde{p}_2 & -2r_1r_2ka_q\tilde{p}_2 & -r_2\tilde{p}_2 \\ eq_1r_1(r_1+r_2) + 2er_1r_2k(q_1\tilde{p}_1 - q_2\tilde{p}_2) & eq_2r_2(r_1+r_2) + 2er_1r_2ka_q(q_2\tilde{p}_2 - q_1\tilde{p}_1) & 0 \end{bmatrix}, \tag{A.3}$$

which we henceforth denote by J for the rest of the present appendix. The characteristic polynomial of (A.3) is

$$|\lambda I - J| = \lambda^3 + a\lambda^2 + b\lambda + c, \tag{A.4}$$

where

$$\begin{aligned} a &= \frac{2k(p_1+a_qp_2)r_1r_2}{r_1+r_2}, \\ b &= \frac{1}{(r_1+r_2)^2}e\left(2kp_1^2q_1r_1^2r_2 + p_2q_2r_2^2(r_1+2a_qkp_2r_1+r_2)\right. \\ &\quad \left. + p_1r_1(-2kp_2q_2r_1r_2 + q_1(r_1^2 + r_1r_2 - 2a_qkp_2r_2^2))\right), \\ c &= \frac{2ekp_1p_2r_1r_2(a_qq_1r_1+q_2r_2)}{r_1+r_2}. \end{aligned} \tag{A.5}$$

According to the Routh–Hurwitz criterion [19,38], the coexistence steady state (2.7) is stable if and only if the coefficients (A.5) satisfy $a > 0$, $c > 0$, and $ab - c > 0$. The conditions $a > 0$ and $c > 0$ are satisfied because of the positivity of the system parameters. To study the third condition, we write $ab - c$ as a polynomial in k. We thereby obtain

$$ab - c = \frac{2r_1r_2}{e(a_qq_1r_1+q_2r_2)^2(r_1+r_2)^2}\left(p_1r_1 - a_qp_2r_2\right)s(k),$$

where

$$s(k) = s_2k^2 + s_1k + s_0, \tag{A.6}$$

with

$$s_0 = \frac{1}{2}e^2 q_1 q_2 r_1 r_2 \log\left(\frac{r_1}{r_2}\right)\left[2a_q q_1 r_1 + 2q_2 r_2 + (-a_q q_1 r_1 + q_2 r_2)\log\left(\frac{r_1}{r_2}\right)\right],$$
$$s_1 = em\left[(r_1+r_2)(a_q^2 q_1^2 r_1^2 - q_2^2 r_2^2) - r_1 r_2(a_q^2 q_1^2 r_1 + q_2^2 r_2 - 3a_q q_1 q_2(r_1+r_2))\log\left(\frac{r_1}{r_2}\right)\right],$$
$$s_2 = 4a_q m^2(a_q q_1 - q_2) r_1 r_2 (r_1 + r_2).$$

Using the steady state (2.7), we see that

$$p_1 r_1 - a_q p_2 r_2 = \frac{a_q k m(r_1^2 - r_2^2) + e(a_q q_1 + q_2) r_1 r_2 \operatorname{arctanh}\left(\frac{r_1 - r_2}{r_1 + r_2}\right)}{ek(a_q q_1 r_1 + q_2 r_2)} > 0.$$

We have thus established that $ab - c > 0 \Leftrightarrow s(k) > 0$.

The value of s at $k = k_0$ is positive:

$$s(k_0) = \frac{e^2 q_1 r_1 (a_q q_1 r_1 + q_2 r_2)^2 \log\left(\frac{r_1}{r_2}\right)\left[r_1 + r_2 + r_2 \log\left(\frac{r_1}{r_2}\right)\right]}{2(r_1 + r_2)} > 0. \tag{A.7}$$

For $a_q \geq q_2/q_1$, the function $s(k)$ is concave up with a positive derivative at k_0. That is,

$$s'(k_0) = em(a_q q_1 r_1 + q_2 r_2)\left[(r_1+r_2)(a_q q_1 r_1 - q_2 r_2) + (3a_q q_1 - q_2) r_1 r_2 \log\left(\frac{r_1}{r_2}\right)\right] > 0. \tag{A.8}$$

Therefore, $a_q \geq q_2/q_1$ implies that $s(k) > 0$ for all $k > k_0$. Finally, if $a_q < q_2/q_1$, we see that $s(k)$ is a downward-opening parabola. Because $s(k_0) > 0$, it follows that s is positive in the interval (k_0, k_1), where

$$k_1 = \frac{-s_1 + \sqrt{s_1^2 - 4s_2 s_0}}{2s_2}. \tag{A.9}$$

□

B Stability of the coexistence steady state in smooth model II

In this appendix, we prove Propositions 2.3 and 2.4. Both of the proofs use the characteristic polynomial of the Jacobian of the second smooth system (2.9). This Jacobian is

$$J = \begin{pmatrix} r_1 - \tilde{q}\tilde{z} & 0 & -\tilde{q}\tilde{p}_1 & -\tilde{p}_1\tilde{z} \\ 0 & r_2 - (1-\tilde{q})\tilde{z} & -(1-\tilde{q})\tilde{p}_2 & \tilde{p}_2\tilde{z} \\ e\tilde{q}\tilde{z} & e(1-\tilde{q})q_2\tilde{z} & e\tilde{q}\tilde{p}_1 + e(1-\tilde{q})q_2\tilde{p}_2 - m & e\tilde{p}_1\tilde{z} - eq_2\tilde{p}_2\tilde{z} \\ \tilde{q}(1-\tilde{q}) & -a_q\tilde{q}(1-\tilde{q}) & 0 & (1-2\tilde{q})(\tilde{p}_1 - a_q\tilde{p}_2) \end{pmatrix}. \tag{B.1}$$

At the coexistence steady state (2.10), the Jacobian (B.1) reduces to

$$J = \begin{pmatrix} 0 & 0 & \frac{-r_1 a_q m}{e(r_1 a_q + r_2 q_2)} & \frac{-a_q m(r_1+r_2)^2}{e(r_1 a_q + r_2 q_2)} \\ 0 & 0 & \frac{-r_2 m}{e(r_1 a_q + r_2 q_2)} & \frac{m(r_1+r_2)^2}{e(r_1 a_q + r_2 q_2)} \\ er_1 & er_2 q_2 & 0 & \frac{e(a_q - q_2)m(r_1+r_2)^2}{e(r_1 a_q + r_2 q_2)} \\ \frac{r_1 r_2}{(r_1+r_2)^2} & \frac{-a_q r_1 r_2}{(r_1+r_2)^2} & 0 & 0 \end{pmatrix}, \tag{B.2}$$

whose eigenvalues are given by the characteristic equation

$$\lambda^4 + \frac{m\left(eq_2 r_2^2 + a_q r_1(er_1 + 2r_2)\right)}{e(a_q r_1 + q_2 r_2)}\lambda^2 + \frac{a_q r_1 r_2 m^2 (a_q - q_2)(r_1 - r_2)}{e(a_q r_1 + q_2 r_2)^2}\lambda + \frac{a_q r_1 r_2 m^2 (r_1 + r_2)}{e(a_q r_1 + q_2 r_2)} = 0. \tag{B.3}$$

Proof. (Proposition 2.3) For $a_q = q_2$, the $\mathcal{O}(\lambda)$ term in equation (B.3) vanishes. Substituting $u = \lambda^2$ then yields

$$u^2 + \frac{m[2r_1r_2 + e(r_1^2 + r_2^2)]}{e(r_1 + r_2)}u + \frac{m^2 r_1 r_2}{e} = 0\,. \tag{B.4}$$

For positive parameter values, the intercept of equation (B.4) is located on the positive vertical axis and equation (B.4) reaches its minimum when $u_i < 0$ (for $i \in \{1, 2\}$). The sign of the discriminant of (B.4) is determined by the following function of e:

$$(r_1^2 + r_2^2)^2 e^2 - 8r_1^2 r_2^2 e + 4 = 0\,, \tag{B.5}$$

which is an upward-opening parabola. The sign of the discriminant of equation (B.5) is thus negative, because

$$64r_1^4 r_2^4 - 16(r_1^4 + 2r_1^2 r_2^2 + r_2^4)r_1^2 r_2^2 = \cdots = -(r_1^2 - r_2^2)^2 < 0\,. \tag{B.6}$$

Because the discriminant of equation (B.5) is negative, it follows that equation (B.5) has no real roots. Therefore, the discriminant of equation (B.4) is always positive, so the two solutions (u_1 and u_2) to equation (B.4) are both real and negative. Consequently, the four eigenvalues λ_j (with $j \in \{1, 2, 3, 4\}$) consist of two complex-conjugate pairs with 0 real part: $\lambda_{1,2} = \pm\sqrt{u_1}i$ and $\lambda_{3,4} = \pm\sqrt{u_2}i$, where u_1 and u_2 satisfy equation (B.4). We thus see that all eigenvalues are purely imaginary. □

Proof. (Proposition 2.4) First, we prove by contradiction that there is at least one eigenvalue with nonzero real part. Assume that all four eigenvalues are purely imaginary. One can then write the characteristic polynomial (B.3) as

$$\chi(\lambda) = \prod_{j=1}^{4}(\lambda - \imath y_j)\,, \quad y_j \in \mathbb{R}\,. \tag{B.7}$$

Expanding χ, we notice that the $\mathcal{O}(\lambda)$ coefficient is

$$\imath(y_1y_2y_3 + y_1y_2y_4 + y_1y_3y_4 + y_2y_3y_4)\,,$$

which is purely imaginary. However, (B.3) has a real coefficient for $\mathcal{O}(\lambda)$ that is nonzero for $a_q \neq q_2$. Therefore, there exists at least one eigenvalue with a nonzero real part.

To complete the proof, we show that there are two eigenvalues whose real parts have opposite signs. Denote the roots of (B.3) by λ_j (with $j \in \{1, 2, 3, 4\}$), and we order the roots so that the real part of λ_1 is nonzero. Because $\sum_{j=1}^{4}\lambda_j = \mathrm{Tr}\,(J) = 0$, at least one of λ_2, λ_3, or λ_4 must have a real part whose sign is opposite to that of λ_1. Consequently, the steady state is unstable. □

C Parameter fitting

Before normalizing both the biweekly data points and the model simulation for these points using the L_2-norm, we add measurement noise (which we choose to be normally distributed between 0 and 0.1) to the model simulation. Thus, when determining the goodness of a fit, we compare each data point to "a noisy" model simulation result for the same point. We simulate the model — using $(p_1(0), p_2(0), z(0)) = (1, 1, 1)$ and $(p_1(0), p_2(0), z(0), q(0)) = (a_q m(r_1 + r_2)/[e(r_1a_q + r_2q_2)], m(r_1 + r_2)/[e(r_1a_q + r_2q_2)], \nu(r_1 + r_2), r_1/(r_1 + r_2))$, respectively, as the initial values for the first smooth model (2.2) and second smooth model (2.9) — for twice the time of spring–summer (i.e., twice from March until August, about 400 days) and discard the first two winter months (i.e., January and February, about 60 days) as a transient. We then align the peak abundances in the data and in the model trajectory, and we then calculate the squared distance between the data and model trajectories:

$$d^2(P) = \frac{\sum_i (P_{\mathrm{data}}(i) - P_*(i))^2}{N}\,, \tag{C.1}$$

where $P_{\mathrm{data}}(i)$ denotes the normalized predator density at the ith selected data point in the generated data, $P_*(i)$ denotes the normalized predator density simulated from the model at the same point, and N is the number of data points.

We iterate the PMC ABC algorithm (see page 987 of [3]) for 10–15 times to collect 2000 candidate parameters (i.e., values for r_1, r_2, m, a_q, and k/ν) at each iteration that yield a distance between the

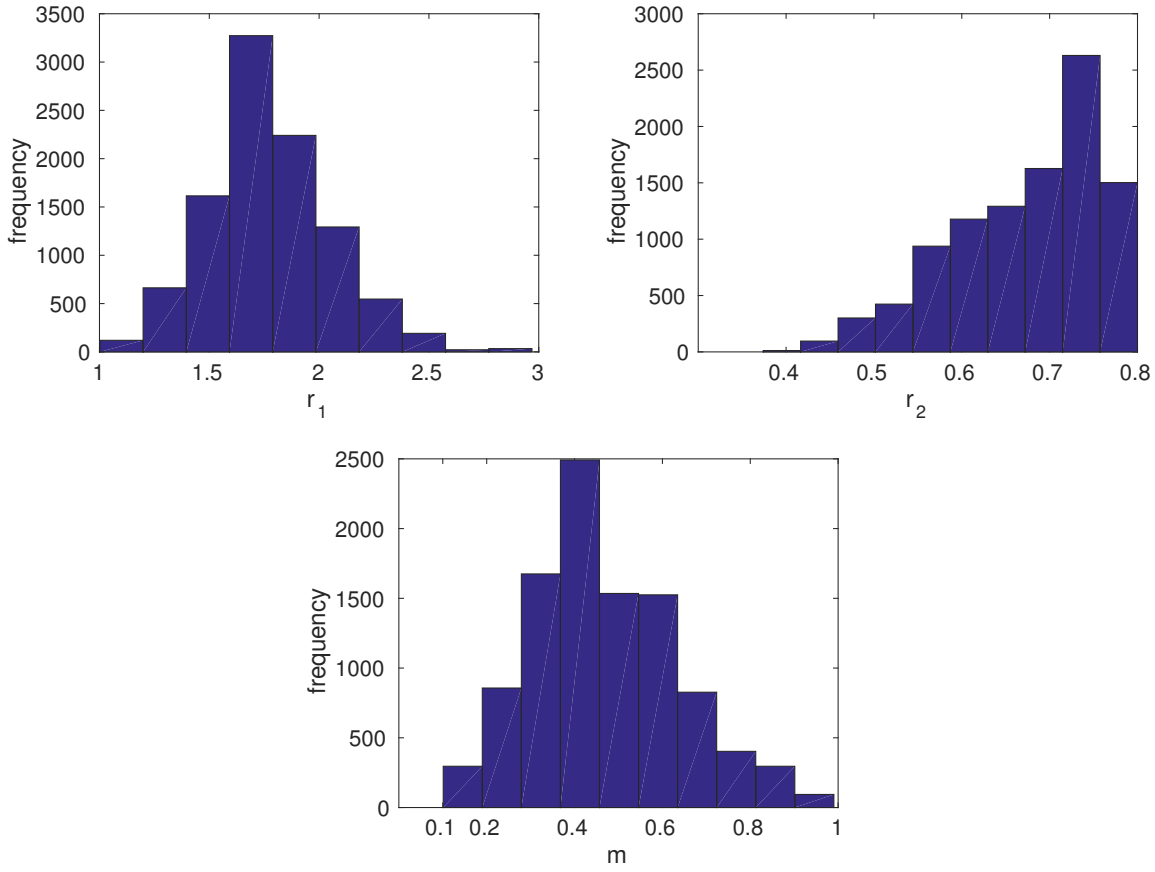

Figure 7: Frequency plots at the strictest tolerance level $\text{Tol}_{15} \approx 0.0292$ using the PMC ABC method [3] for the parameters r_1, r_2, and m of the first smooth model (2.2) and the unselective predator group in year 1998. For frequency plots of k and a_q, see the middle and bottom right panels of Figure 2 in the main text. The frequency plot represents a random weighted sample (of size 10000) from the parameter values at the strictest tolerance level.

perturbed model prediction and the data that is smaller than a given tolerance threshold. From the literature (see, e.g., [48]) and simulating the models numerically, we determine maximum and minimum values for each parameter and assume that the parameters in the first iteration are distributed uniformly between these values. Therefore, for the first smooth system, we assume the following prior distributions: $r_1 \sim \mathcal{U}(1,3)$, $r_2 \sim \mathcal{U}(0.01,0.8)$, $m \sim \mathcal{U}(0.1,1)$, $a_q \sim \mathcal{U}(0.01,2)$, and $k \sim \mathcal{U}(1,100)$. For the second smooth system, we assume that $m \sim \mathcal{U}(0.05,1)$ and $\nu \sim \mathcal{U}(1.1,5)$. We determine a decreasing sequence of tolerance thresholds by setting the threshold of the subsequent iteration to be either (1) the distance between the data and the model prediction of the best 10% quantile of the current step or (2) equal to the tolerance threshold of the current step (if the distance of the 10% quantile is larger than the current tolerance threshold). Based on several test runs, we choose the following initial tolerance levels. For the first smooth dynamical system (2.2), we choose $\text{Tol}_1 \approx 0.022$ for a selective predator in 1991, $\text{Tol}_1 \approx 0.038$ for an unselective predator in 1991, $\text{Tol}_1 \approx 0.0525$ for a selective predator in 1998, and $\text{Tol}_1 \approx 0.0475$ for an unselective predator in 1998. For the second smooth dynamical system (2.9), we choose $\text{Tol}_1 \approx 0.02$ for a selective predator in 1991, $\text{Tol}_1 \approx 0.03$ for an unselective predator in 1991, $\text{Tol}_1 \approx 0.0375$ for a selective predator in 1998, and $\text{Tol}_1 \approx 0.032$ for an unselective predator in 1998. In Figure 7, we show an example of frequency plots at the strictest tolerance level for other parameters than the ones that we reported in Section 3.

References

[1] D. S. Abbot, A. Voigt, and D. Koll, *The Jormungand global climate state and implications for Neoproterozoic glaciations*, Journal of Geophysical Research: Atmospheres (1984–2012), 116 (2011),

p. D18103.

[2] P. A. Abrams and H. Matsuda, *Population dynamical consequences of reduced predator switching at low total prey densities*, Population Ecology, 45 (2003), pp. 175–185.

[3] M. A. Beaumont, J.-M. Cornuet, J.-M. Marin, and C. P. Robert, *Adaptive approximate Bayesian computation*, Biometrika, 96 (2009), pp. 983–990.

[4] M. Broucke, C. Pugh, and S. N. Simić, *Structural stability of piecewise smooth systems*, Journal of Computational and Applied Mathematics, 20 (2001), pp. 51–89.

[5] G. Casey, H. De Jong, and G. J.-L., *Piecewise-linear models of genetic regulatory networks: Equilibria and their stability*, Journal of Mathematical Biology, 52 (2006), pp. 27–56.

[6] A. R. Champneys and M. di Bernardo, *Piecewise smooth dynamical systems*, Scholarpedia 3(9):4041, 2008. `http://www.scholarpedia.org/article/Piecewise_smooth_dynamical_systems/` Accessed: 12-06-2013.

[7] A. Colombo, M. di Bernardo, S. J. Hogan, and M. R. Jeffrey, *Bifurcations of piecewise smooth flows: Perspectives, methodologies and open problems*, Physica D, 241 (2012), pp. 1845–1860.

[8] M. di Bernardo, C. J. Budd, A. R. Champneys, and P. Kowalczyk, *Piecewise-Smooth Dynamical Systems*, Springer, 2008.

[9] M. Di Bernardo, K. H. Johansson, and F. Vasca, *Self-oscillations and sliding in relay feedback systems: Symmetry and bifurcations*, International Journal of Bifurcation and Chaos, 11 (2001), pp. 1121–1140.

[10] G. F. Fussmann, M. Loreau, and P. A. Abrams, *Eco-evolutionary dynamics of communities and ecosystems*, Functional Ecology, 21 (2007), pp. 465–477.

[11] G. F. Gause, N. P. Smaragdova, and A. A. Witt, *Further studies of interaction between predators and prey*, Journal of Animal Ecology, 5 (1936), pp. 1–18.

[12] L. Glass, *Classification of biological networks by their qualitative dynamics*, Journal of Theoretical Biology, 54 (1975), pp. 85–107.

[13] J. Guckenheimer and P. Holmes, *Nonlinear Oscillations, Dynamical Systems, and Bifurcations of Vector Fields*, Springer, 1996.

[14] T. Hiltunen, S. P. Ellner, G. Hooker, L. E. Jones, and N. G. Hairston Jr, *Eco-evolutionary dynamics in a three-species food web with intraguild predation: intriguingly complex*, Advances in Ecological Research, 50 (2014), pp. 41–74.

[15] E. J. Hinch, *Perturbation Methods*, Cambridge University Press, 1991.

[16] N. Hinrichs, M. Oestreich, and K. Popp, *On the modelling of friction oscillators*, Journal of sound and Vibration, 216 (1998), pp. 435–459.

[17] S. J. Hogan, *On the dynamics of rigid-block motion under harmonic forcing*, 425 (1989), pp. 441–476.

[18] C. S. Holling, *The functional response of predators to prey density and its role in mimicry and population regulation*, Memoirs of the Entomological Society of Canada, 97 (1965), pp. 5–60.

[19] A. Hurwitz, *Ueber die bedingungen, unter welchen eine gleichung nur wurzeln mit negativen reellen theilen besitzt*, Matematische Annalen, (1895), pp. 273–284.

[20] T. M. Inc., 2014. Natick, Massachusetts.

[21] M. R. Jeffrey, *Nondeterminism in the limit of nonsmooth dynamics*, Physical Review Letters, 106 (2011), p. 254103.

[22] ——, *Hidden dynamics in models of discontinuity and switching*, Physica D, 273–274 (2014), pp. 34–45.

[23] ——, *Hidden degeneracies in piecewise smooth dynamical systems*, International Journal of Bifurcation and Chaos, 26 (2016), pp. 1–18.

[24] ——, *Smoothing tautologies, hidden dynamics, and sigmoid asymptotics in piecewise smooth systems*, Chaos, 25 (2016), pp. 1–11.

[25] C. K. R. T. Jones, *Geometric Singular Perturbation Theory*, Cambridge University Press, 1991.

[26] S. A. Kelly, T. M. Panhuis, and A. M. Stoehr, *Phenotypic plasticity: Molecular mechanisms and adaptive significance*, Comprehensive Physiology, 2 (2012), pp. 1417–1439.

[27] V. Křivan, *Optimal foraging and predator–prey dynamics I*, Theoretical Population Biology, 49 (1996), pp. 265–290.

[28] C. Kuehn, *Multiple Time Scale Dynamics*, Springer-Verlag, 2015.

[29] V. Křivan and J. Eisner, *Optimal foraging and predator–prey dynamics, III*, Theoretical Population Biology, 63 (2003), pp. 269–279.

[30] V. Křivan and A. Sikder, *Optimal foraging and predator–prey dynamics II*, Theoretical Population Biology, 55 (1999), pp. 111–126.

[31] J. Leifeld, K. Hill, and A. Roberts, *Persistence of saddle behavior in the nonsmooth limit of smooth dynamical systems*, arXiv:1504.04671 [math.DS], (2015).

[32] H. P. McKean, *Nagumo's equation*, Advances in Mathematics, 4 (1970), pp. 209–223.

[33] H. Müller and A. Schlegel, *Responses of three freshwater planktonic ciliates with different feeding modes to cryptophyte and diatom prey*, Aquatic Microbial Ecology, 17 (1999), pp. 49–60.

[34] W. W. Murdoch, *Switching in general predators: Experiments on prey specificity and stability of prey populations*, Ecological Monographs, 39 (1969), pp. 335–354.

[35] S. H. Piltz, M. A. Porter, and P. K. Maini, *Prey switching with a linear preference trade-off*, SIAM Journal on Applied Dynamical Systems, 13 (2014), pp. 658–682.

[36] S. H. Piltz, F. Veerman, P. K. Maini, and M. A. Porter, *A predator–2 prey fast–slow dynamical system for rapid predator evolution*, 2016. arXiv:1603.09076.

[37] D. M. Post, M. E. Conners, and D. S. Goldberg, *Prey preference by a top predator and the stability of linked food chains*, Ecology, 81 (2000), pp. 8–14.

[38] E. J. Routh, *A treatise on the stability of a given state of motion, particularly steady motion*, 1877. Macmillan and Co.

[39] M. Shimada, Y. Ishii, and H. Shibao, *Rapid adaptation: A new dimension for evolutionary perspectives in ecology*, Population Ecology, 52 (2010), pp. 5–14.

[40] U. Sommer, R. Adrian, L. D. S. Domis, J. J. Elser, U. Gaedke, B. Ibelings, E. Jeppesen, M. Lurling, J. C. Molinero, W. M. Mooij, E. van Donk, and M. Winder, *Beyond the Plankton Ecology Group (PEG) model: Mechanisms driving plankton succession*, Annual Review of Ecology, Evolution, and Systematics, 43 (2012), pp. 429–448.

[41] J. Sotomayor and M. A. Teixeira, *Regularization of discontinuous vector fields*, in International Conference on Differential Equations, Lisboa, Equadiff 95, 1996, 1996, pp. 207–223.

[42] D. W. Stephens and J. R. Krebs, *Foraging Theory*, Princeton University Press, 1986.

[43] H. Stommel, *Thermohaline convection with two stable regimes of flow*, Tellus, 13 (1961), pp. 224–230.

[44] M. A. Teixeira and P. R. da Silva, *Regularization and singular perturbation techniques for non-smooth systems*, Physica D, 241 (2012), pp. 1948–1955.

[45] K. Tirok and U. Gaedke, *Spring weather determines the relative importance of ciliates, rotifers and crustaceans for the initiation of the clear-water phase in a large, deep lake*, Journal of Plankton Research, 28 (2006), pp. 361–373.

[46] ——, *Regulation of planktonic ciliate dynamics and functional composition during spring in Lake Constance*, Aquatic Microbial Ecology, 49 (2007), pp. 87–100.

[47] ——, *The effect of irradiance, vertical mixing and temperature on spring phytoplankton dynamics under climate change: Long-term observations and model analysis*, Oecologia, 150 (2007), pp. 625–642.

[48] ——, *Internally driven alternation of functional traits in a multispecies predator–prey system*, Ecology, 91 (2010), pp. 1748–1762.

[49] T. Toni, D. Welch, N. Strelkowa, A. Ipsen, and M. P. Stumpf, *Approximate Bayesian computation scheme for parameter inference and model selection in dynamical systems*, Journal of the Royal Society Interface, 6 (2009), pp. 187–202.

[50] E. van Leeuwen, Å. Brännström, V. A. A. Jansen, U. Dieckmann, and A. G. Rossberg, *A generalized functional response for predators that switch between multiple prey species*, Journal of Theoretical Biology, 328 (2013), pp. 89–98.

[51] E. van Leeuwen, V. A. A. Jansen, and P. W. Bright, *How population dynamics shape the functional response in a one-predator–two-prey system*, Ecology, 88 (2007), pp. 1571–1581.

[52] P. Verity, *Feeding in planktonic protozoans: Evidence for nonrandom acquisition of prey*, The Journal of Protozoology, 38 (1991), pp. 69–76.

[53] M. Yamamichi, T. Yoshida, and A. Sasaki, *Comparing the effects of rapid evolution and phenotypic plasticity on predator–prey dynamics*, The American Naturalist, 178 (2011), pp. 287–304.